

## Light dependence of selenium uptake by phytoplankton and implications for predicting selenium incorporation into food webs

*Stephen B. Baines and Nicholas S. Fisher*

Marine Sciences Research Center, Stony Brook University, Stony Brook, New York 11794-5000

*Martina A. Doblin, Gregory A. Cutter, and Lynda S. Cutter*

Ocean, Earth, and Atmospheric Sciences, Old Dominion University, 4600 Elkhorn Avenue, Norfolk, Virginia 23529

*Brian Cole*

U.S. Geological Survey, 345 Middlefield Road, Menlo Park, California 94025-3591

### *Abstract*

The potentially toxic element selenium is first concentrated from solution to a large but highly variable degree by algae and bacteria before being passed on to consumers. The large loads of abiotic and detrital suspended particles often present in rivers and estuaries may obscure spatial and temporal patterns in Se concentrations at the base of the food web. We used radiotracers to estimate uptake of both selenite (Se(IV)) and C by intact plankton communities at two sites in the Sacramento/San Joaquin River Delta. Our goals were to determine (1) whether C and Se(IV) uptake were coupled, (2) the role of bacteria in Se(IV) uptake, and (3) the Se:C uptake ratio of newly produced organic material. Se(IV) uptake, like C uptake, was strongly related to irradiance. The shapes of both relationships were very similar except that at least 42–56% of Se(IV) uptake occurred in the dark, whereas C uptake in the dark was negligible. Of this dark Se(IV) uptake, 34–67% occurred in the 0.2–1.0- $\mu\text{m}$  size fraction, indicating significant uptake by bacteria. In addition to dark uptake, total Se(IV) uptake consisted of a light-driven component that was in fixed proportion to C uptake. Our estimates of daily areal Se(IV):C uptake ratios agreed very well with particulate Se:C measured at a site dominated by phytoplankton biomass. Estimates of bacterial Se:C were 2.4–13 times higher than for the phytoplankton, suggesting that bacterivores may be exposed to higher dietary Se concentrations than herbivores.

Depending on its concentration, selenium (Se) can be either a serious toxic contaminant or a limiting nutrient for aquatic organisms (Brown and Shrift 1982; Harrison et al. 1988). Se toxicity is a potential problem in many ecosystems where an arid climate and high Se soil concentrations combine to concentrate Se in surface and ground waters (Lauchli 1993). Anthropogenic inputs in the form of industrial waste (Bowie et al. 1996) and atmospheric deposition of airborne Se-containing particles released from coal-burning power plants (Cutter and Cutter 1998) are also important sources to some aquatic environments. Understanding the spatial and temporal variability in the selenium concentration in aquatic organisms has been of particular concern in freshwater bodies of central California and other western states, where a combination of naturally high Se concentrations in the soil, irrigation practices, and agricultural management strategies has led to instances of catastrophic poisoning (Presser 1994; Presser et al. 1994).

To understand and predict Se concentration in consumer organisms, it is necessary to know the concentration of Se in organisms that form the base of the food web (Fisher and

Reinfelder 1995). Almost all of the Se in aquatic consumers derives from dietary Se (Reinfelder and Fisher 1991; Luoma et al. 1992; Wang et al. 1996). This dietary Se derives ultimately from phytoplankton and bacteria, which concentrate Se from solution by up to 100,000-fold, although the degree of concentration may vary several orders of magnitude among algal species (Baines and Fisher 2001). Se in algae and bacteria, primarily reduced Se(-II) contained in selenoaminoacids (methionine and cysteine) in free or combined form (Wrench 1978; Foda et al. 1983; Bottino et al. 1984), is readily assimilated from algae by herbivores and may even be biomagnified 2–4 times with trophic transfer (Liu et al. 1987), although such biomagnification is not always observed (Reinfelder et al. 1998; Baines et al. 2002). Bacteria are also clearly involved in concentrating dissolved Se into the particulate fraction (Foda et al. 1983; Riedel and Sanders 1996). We might expect that bacteria have higher Se concentrations than algae given that their lower C:N ratios imply higher relative protein content (Sterner and Elser 2002). Since bacteria:phytoplankton biomass ratios can vary significantly spatially and temporally in aquatic ecosystems (Cole et al. 1988; Findlay et al. 1991), such differences in Se content could explain patterns in consumer Se burdens.

Because the net uptake of Se and C by algae is linked through the primary production of organic matter and cell growth (Baines and Fisher 2001), we hypothesize that Se uptake, like inorganic C uptake, is related to irradiance. Time- and depth-integrated C uptake is typically measured

### *Acknowledgments*

We thank L. Lucas, R. Stewart, S. Meseck, T. Shraga, and C. Lopez for help with sampling and data acquisition, and Sam Luoma for help with the radioisotope experiments and providing access to equipment for radiotracer analyses. This project was supported by the Calfed Bay/Delta program (02WRAG0003). This is Marine Science Research Center contribution 1267.

by modeling the response of C fixation to light then integrating the model predictions over the appropriate light and time fields (Falkowski and Raven 1997). Depth-integrated daily Se uptake may be estimated similarly based on measurements of inorganic  $^{75}\text{Se}$  uptake at different light levels. Alternatively, if Se and C uptake scale proportionately with light levels, a measurement of the uptake ratio at one light level combined with a measure of integrated C fixation may be all that is needed to get a reasonable estimate of local exposure of higher trophic levels to Se via algal food. By coupling these measurements with bacterial production estimates, Se:C ratios for both algae and bacteria could be determined. Such an approach would measure the Se:C ratio of only the living cells that form the base of the food web and not of the abiotic material and nonliving detritus. Non-living particles can dominate the suspended particulate matter in rivers and estuaries, potentially causing chemical measurements of the Se:C ratio in suspended particles to differ from the Se:C of the material that is either ingested or readily assimilated by bivalves and crustaceans.

As part of a large interdisciplinary study of C and Se transformations and transport in the Sacramento/San Joaquin River delta in California, we measured uptake of  $^{14}\text{C}$ -labeled bicarbonate by phytoplankton and uptake of  $^{75}\text{Se}$ -labeled selenite ( $\text{Se(IV)}$ ) by phytoplankton and bacteria. These experiments focused on uptake of selenite, since this form is generally considered most bioavailable (Riedel et al. 1991; Hu et al. 1997). We addressed three specific questions: (1) What fraction of the selenite uptake onto particles is the result of bacterial activity? (2) How is selenite uptake related to incident irradiance? (3) Does the  $\text{Se(IV)}:\text{C}$  uptake ratio vary with irradiance or production? We also attempted to develop a model that relates daily depth-integrated C uptake to Se uptake in bacteria and phytoplankton. Model predictions are then compared to measurements of Se:C in biogenic particles and the variability in dissolved and particulate Se concentrations at a eutrophic site in the Sacramento/San Joaquin Delta.

## Materials and methods

**Study site**—Measurements were conducted using water collected in or near Mildred Island, a former agricultural tract that because of subsidence lay below river level until it flooded during intense El Niño rains in 1983 (Fig. 1). Mildred Island is a 4.1-km<sup>2</sup> body of water separated from the river channels that surround it by the remnants of an encircling levee. Hydrologic communication between the body of Mildred Island and the channel is primarily as tidal flux through a major gap (~170 m wide and ~18 m deep) in the northeast section of the levee, and another smaller gap in the south (~18 m wide and ~1 m deep), although many smaller gaps exist elsewhere (Monsen et al. 2002). Average flushing time within Mildred Island is 2.4–8.8 d, i.e., much longer than in the surrounding channel but very short compared to a typical lake. Retention is also spatially variable, ranging from 1 to >160 h. The southeastern portion of the water body is particularly isolated from the channel, resulting in diel thermal stratification and a large accumulation of

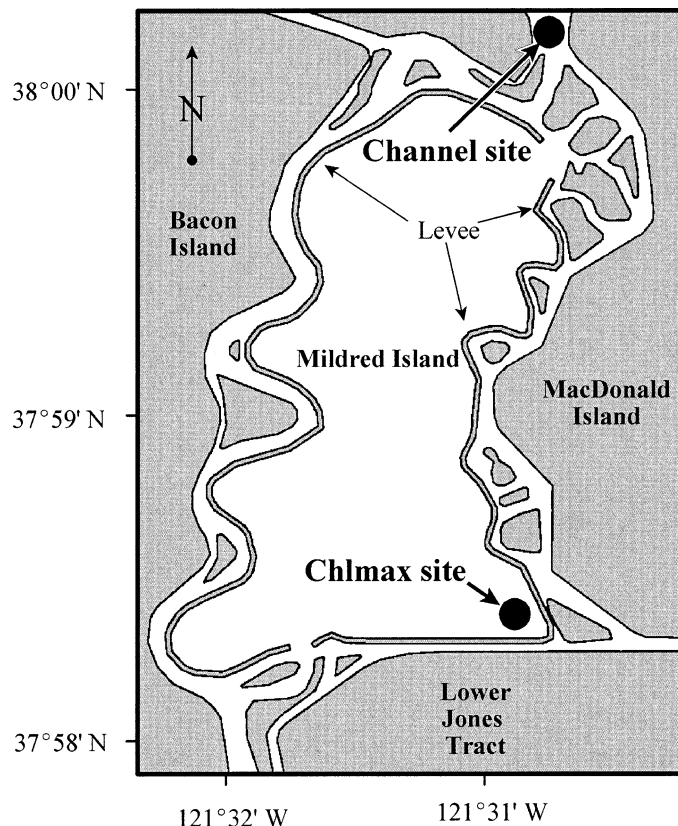


Fig. 1. Map of the sampling site. Gray areas represent dry land or emergent vegetation; white areas, open water. Sampling sites are indicated by the dark circles. Chl max site = site of maximum chlorophyll.

algal biomass every day (Lucas et al. 2002). While the chlorophyll *a* concentration in the surrounding river channel ranged between 2.3 and 3.1  $\mu\text{g L}^{-1}$ , in the southeastern section of Mildred Island concentrations ranged from 12.4  $\mu\text{g L}^{-1}$  in the early morning to 30  $\mu\text{g L}^{-1}$  in the early evening (Table 1) during the course of this experiment.

**Sampling**—Water for the uptake experiments was collected from two sites. One represented the high-chlorophyll, long residence time conditions in the southeastern corner of Mildred Island (Chl max) and the other the low-chlorophyll, short residence time conditions of the adjacent channel (Channel; Fig. 1). Water samples for use in the experiments were collected using a trace-element clean Go Flo bottle from a depth of 1 m. Three to five liters of water were then drained into a darkened 20-liter collapsible plastic cubitainer via a funnel fitted with an 100- $\mu\text{m}$  mesh nitex netting to remove large grazers. The cubitainer had been acid washed three times with trace metal grade 10% HCl and with ambient water prior to sampling. These samples were immediately transported to the onshore experimental site (transit time ~20 min). The length and intensive nature of the experiments limited us to four experimental incubations, two each from the Chl max and Channel sites. To encompass the range of diel variability, one set of samples from each site

Table 1. Conditions at the time of the Se and C uptake experiments.

Period	Site	Time of sampling (h)	Experiment duration (h)	Sampling intervals	Ambient DIC ( $\mu\text{mol L}^{-1}$ )	Initial Chl ( $\mu\text{g (Chl } a)^{-1} \text{ L}^{-1}$ )	Ambient Se(IV) ( $\text{nmol L}^{-1}$ )
Morning	Channel	0742	7.6	4	1049	2.3	0.29
Evening	Channel	1644	6.1	5	692	3.1	0.24
Morning	Chl max	1109	8.2	4	881	12.4	0.41
Evening	Chl max	2044	6.9	5	760	30.0	0.28

was collected in the morning and another in the late afternoon/early evening (see Table 1 for exact time of collection).

These two sites and a third intermediate site near the mouth of the main levee break were also sampled for determination of particulate and dissolved Se concentrations, dissolved Se speciation, chlorophyll *a* concentration, and particulate organic carbon and nitrogen. These results are described more fully elsewhere (Martina Doblin pers. comm.). Samples for determination of Se in dissolved and particulate fractions were collected immediately after collection of samples for uptake experiments. Samples to determine Se variability were collected every 3 h over a 2-d period. In addition, at five times over the first 24 h of the experiment, 250-ml samples were collected from the Chl max site in Mildred Island and preserved with Lugol's solution for microscopic determination of the phytoplankton and protozoan species composition. One such sample was also collected from the channel.

*Chemical and phytoplankton characterization*—Water samples for total particulate selenium determinations were directly pressure filtered (Go Flo bottle pressurized with 0.5 atm.  $\text{N}_2$  and >1.5 liters of water passed through filter apparatus) onto preweighed 0.4- $\mu\text{m}$ , 142-mm (outside diameter) polycarbonate filters that were frozen immediately upon completion of the filtration. Water passing through the filter was placed in 1-liter borosilicate glass bottles with Teflon-lined caps and acidified to pH 1.6 with HCl; these were stored in the dark until analysis. Experience has shown that storage in borosilicate glass bottles with Teflon-lined caps and 1.0 M HCl acidification (used in preference to  $\text{HNO}_3$  because of potential nitrite interference during Se determinations—see Cutter 1983) preserves the Se speciation and results in good analytical accuracy and precision. Dissolved selenite (Se(IV)), selenate (Se(VI)), and organic selenide (org Se(-II)) were determined using the selective hydride generation procedures described by Cutter (1978, 1982, 1983) and included triplicate analyses and the use of the standard additions method of calibration.

After drying the filters at 40°C and reweighing (to determine total suspended matter), suspended particles were solubilized using a multistep wet oxidation (Cutter 1985). Total dissolved selenium was then determined in treated digest solutions using the same dissolved selenium method as above, with a detection limit of 1 pmol  $\text{L}^{-1}$  and an average coefficient of variation of 4.1% at a concentration of 0.1 nmol  $\text{L}^{-1}$ . The accuracy of these digestions was assured using the standard additions method of calibration and the parallel digestion/analysis of a standard reference material (Na-

tional Institute of Standards and Technology 1566b Oyster Tissue). Suspended particulate organic carbon and nitrogen were determined using a Carlo Erba ANA 1500 elemental analyzer for water samples filtered onto solvent-cleaned Whatman GF/F filters (13 mm outside diameter) (Cutter and Radford-Knoery 1991).

Samples for chlorophyll determination were filtered onto 25-mm Gelman AE glass fiber filters under low pressure (<125 mm Hg). Filters were kept frozen until analysis. Chlorophyll and phaeophytin were measured using the fluorometric methods of Arar and Collins (1997) with slight modifications. Filters were extracted in 90% acetone at 4°C overnight. After removing particulates from the sample by centrifugation, fluorescence was measured on room temperature samples using a Turner Designs model 10 fluorometer. The samples were acidified with 1 N HCl, and fluorescence was measured again. Chlorophyll *a* and phaeophytin were estimated from these two fluorescence measurements. In addition to chlorophyll, Dissolved inorganic carbon (DIC) was measured using titration to a colorimetric end point (Furutani et al. 1984). Phytoplankton and protozoan community composition were determined for the Lugol's preserved samples using the Utermöhl settling technique.

*Coupled Se:C uptake experiments*—Uptake of Se and C was measured in incubators designed to provide a range of irradiances under controlled temperature conditions. The apparatus consisted of a rectangular opaque acrylic chamber with a transparent face plate at one end. Each chamber held 12 disposable 250-ml clear sterile polyethylene cell culture flasks with Teflon-lined caps aligned in a row facing the transparent face plate. The last two flasks were made opaque by painting them with multiple coats of flat black paint. All of the flasks, none of which had been used prior to this experiment, were rinsed with 10% trace metal grade HCl followed by 18- $\mu\text{m}$  Milli-Q deionized water. To prevent atmospheric Se contamination and loss of radiolabel, flasks were kept closed throughout the experiment except during sampling. A 150 W flood lamp was directed toward the transparent face of the chamber to provide the light source. The photosynthetically active radiation (PAR) measured in the center of the last clear flask was 8% of that in the flask nearest the transparent face plate as measured with a spherical quantum scalar irradiance meter (Biospherical Instruments model QSL 2001). This chamber was connected via polyvinyl chloride (PVC) pipe to a 20-liter reservoir of water. The water was maintained at 25°C  $\pm$  1°C (the ambient temperature) by recirculating it through a 1/5-hp aquarium chiller. Cooling water was pumped at a rate of 10  $\text{L min}^{-1}$

from the reservoir to the incubation apparatus near the clear face plate. Return flow from the incubation chamber to the reservoir was by gravity.

For each of two replicate incubation chambers, 125-ml aliquots were taken from a mixed bulk sample cubitainer and distributed to seven of the 250-ml cell culture flasks—five clear flasks exposed to 100%, 54%, 30%, 15%, and 8% of the radiation incident on the first flask, and the two opaque flasks. To account for abiotic Se(IV) uptake, one of the dark flasks was used as a killed control; the sample in this flask was heated in a microwave oven for two 2.5-min intervals, being careful not to allow boiling (Keller et al. 1988). The chamber and flasks were allowed to equilibrate for 1 h. We then added 555 Bq of  $^{75}\text{Se}$ -labeled sodium selenite (in 0.1 N HCl) followed by 46.25 kBq of  $^{14}\text{C}$ -labeled sodium bicarbonate to each flask, taking care to offset the HCl additions resulting from the isotope additions with equimolar additions of NaOH before adding the radiolabeled bicarbonate. The contents of each flask were mixed, and then 1-ml samples were immediately taken for analysis of initial isotope additions. The concentration of added Se was 0.03 nmol L<sup>-1</sup>, which was <15% of the ambient selenite concentration.

The dual and single radiotracer experiments were conducted in the morning and evening to determine whether the relationships between light and the uptake of Se(IV) and C changed over the course of the day. The time course of incorporation of  $^{14}\text{C}$  and  $^{75}\text{Se}$  into the particulate fraction was followed to determine whether uptake was linear over time. Aliquots of 10 ml from each flask were collected at four times over 7–8 h in the morning experiments and five times over 6–7 h in the evening experiments. The aliquots were filtered through 0.2- $\mu\text{m}$  polycarbonate membrane filters (Poretics) and then rinsed with an equal volume of unlabeled water from Mildred Island. For the morning incubations, we also filtered samples through 1.0- $\mu\text{m}$  pore size filters to allow estimates of the uptake into the predominantly bacterial size fraction (0.2–1.0  $\mu\text{m}$ ) by difference. Simultaneously, samples of 1 ml were collected to estimate total radioactivity in solution. All samples were placed in scintillation vials; those containing a filter received 1 ml of 1.2 N HCl to eliminate any residual inorganic carbon, while liquid samples received 3 ml of 1 N NaOH to prevent loss of  $^{14}\text{C}$ .

There was also a parallel set of experiments measuring only primary productivity, as indicated by uptake of  $^{14}\text{C}$ . In these experiments primary production was measured with short-term incubations of  $\text{NaH}^{14}\text{CO}_3$ -spiked water samples in a commercially produced photosynthetron (Lewis and Smith 1983) that provided a range of irradiance from darkness to full sunlight. A 740-kBq addition of  $\text{NaH}^{14}\text{CO}_3$  was added to a 50-ml water sample. Then, 2-ml aliquots of the radioactively labeled sample were dispensed into each of 17 liquid scintillation vials. The 2-ml aliquots were incubated for 30 min, then acidified with 0.4 ml of 0.5 N HCl and agitated in a hood for 1 h to stop carbon uptake and purge the unincorporated  $\text{NaH}^{14}\text{CO}_3$  from the sample. Abiotic uptake of  $\text{NaH}^{14}\text{CO}_3$  was determined by acidifying triplicate samples immediately after the  $\text{NaH}^{14}\text{CO}_3$  addition. The measure of abiotic  $^{14}\text{C}$  uptake was subtracted from the activity of each incubated sample.

Dual isotope samples were prepared for gamma and beta

emission analysis within 24 to 48 h after collection in the field. Vials with filters in them were swirled, opened, and placed in a hood for 3 h to vent any residual  $^{14}\text{CO}_2$  produced by acidification. Afterward, 3 ml of 1 N NaOH were added to buffer the scintillant, thereby minimizing pH-related variability in counting efficiency. Ten milliliters of scintillant (Optima-Gold, Perkin Elmer) were then added and the contents homogenized by vigorous shaking. The vials were analyzed for  $^{75}\text{Se}$  by counting gamma emissions for 10 min at 278 keV on an autosampling Wallac 1480 Wizard 3 fitted with a NaI(Tl) well detector. Uptake into particles was expressed as a percentage of the total radioactivity in suspension. Prior to analysis of beta emissions, the vials with scintillant were allowed to sit in the dark for 1 d. Beta emissions were analyzed by liquid scintillation counting for 10 min using the external standards ratio method for quench correction. Beta emissions by  $^{75}\text{Se}$  were found to contribute a negligible amount (<5%) to estimates of  $^{14}\text{C}$  beta emissions. From the assays of gamma and beta radioactivity in the dissolved and particulate phases, we determined the fraction of added  $^{75}\text{Se}$  and  $^{14}\text{C}$  radiotracer taken up into particles at each sampling point.

*Data analysis*—Se(IV) and C uptake in the dual isotope experiments were corrected for abiotic uptake by subtracting the amounts of particulate  $^{75}\text{Se}$  and  $^{14}\text{C}$  in the dark killed flasks (assumed to reflect abiotic uptake) from the amounts observed in each of the other flasks. Only the corrected data from the live flasks are presented and used in statistical tests. For the morning incubations, uptake into the bacterial size fractions was estimated by subtracting  $^{75}\text{Se}$  and  $^{14}\text{C}$  observed in the >1- $\mu\text{m}$  fraction from that in the >0.2- $\mu\text{m}$  fraction. Initially we expressed uptake as a percentage of the initial dissolved isotope pool taken up. To estimate the mean C uptake rates (% h<sup>-1</sup>) at a particular light level, we averaged the rates measured over each interval of the time series. We were not able to use a similar approach for all of the Se(IV) uptake experiments because low counts in the initial phase of some of the treatments resulted in poor analytical statistics and high variability. Instead, we took the final value for percent Se(IV) uptake into particles and divided by the length of entire incubation, assuming uptake was linear with time. Absolute uptake on a pmol L<sup>-1</sup> h<sup>-1</sup> basis was calculated by multiplying the percentage of isotope taken up into particles per hour by the total (ambient + added) Se(IV) or DIC concentrations in pmol L<sup>-1</sup> (Table 1).

Se(IV) uptake and C uptake were normalized to chlorophyll to remove the effects of variations in algal biomass. Chlorophyll-specific primary production,  $P^b$ , and Se(IV) uptake,  $u\text{Se(IV)}^b$ , were related to irradiance ( $I$ ,  $\mu\text{mol quanta m}^{-2} \text{ s}^{-1}$ ) by nonlinear least-squares regression using the Levenberg–Marquardt iterative search algorithm within SigmaPlot 7.1 (SPSS). The model used was a hyperbolic tangent,  $U^b = y + \frac{U_{\text{max}}^b}{1 + \tanh(I \times I_k^{-1})}$ , where  $U$  stands for either primary production or Se(IV) uptake,  $U^b$  is the biomass specific uptake,  $U_{\text{max}}^b$  is the maximum chlorophyll-specific uptake, and  $I_k$  is the shape parameter for the curve (Jassby and Platt 1976). Dark uptake was presumed to equal the y-intercepts of these regressions. The uptake of Se(IV) in the live dark flasks was always within 10% of these y-intercepts.

Table 2. Fraction of the phytoplankton biovolume contributed by the dominant phytoplankton species during the experiments. Only species contributing more than 5% of the community biovolume at one or more sites are included.

Group	Major species	Chl max		Channel (both)
		Morning	Evening	
Bacillariophyceae	<i>Cyclotella atomus</i>	39.7	50.2	86.3
	<i>Skeletonema potamus</i>	7.5	19.4	
Cryptophyceae	<i>Teleaulax amphioxiea</i>	10.5		2.7
	<i>Plagioselmis</i> sp.	22.3	15.8	1.2
Cyanophyceae	<i>Cyanobium</i> sp.	12.3	7.7	5.0

Absolute uptake of C and Se(IV) at a specific depth and time was estimated by substituting the equation relating  $I$  to depth ( $z$ ),  $I_z = I_0 e^{-az}$ , into the hyperbolic tangent model and multiplying the result by the chlorophyll concentration.

$$U_{t,z} = \{y + U_{\max,t}^b \tanh[(-I_0 e^{-az} I_k^{-1})]\} \text{Chl}_t \quad (1)$$

where  $\text{Chl}_t$ ,  $I_0$ ,  $a$ , and  $z$  are the chlorophyll  $a$  concentration ( $\text{mg Chl } a \text{ m}^{-3}$ ), the surface irradiance ( $\mu\text{mol photons m}^{-2} \text{ s}^{-1}$ ), the light extinction coefficient at time  $t$  ( $\% \text{ m}^{-1}$ ), and the depth (m) below the surface, respectively. Depth-integrated primary production was estimated for 0.1-h intervals over the course of the day by taking the definite integral of Eq. 1 between the surface and the depth of the water column (5 m). Because chlorophyll concentrations varied 2–3 fold over the diel cycle, we linearly interpolated chlorophyll  $a$  concentrations at each point,  $t$ , between the trihourly chlorophyll measurements. The light extinction coefficient at the Chl max site, where phytoplankton dominated turbidity, was estimated from chlorophyll concentration by using Carlson's regression (Carlson 1977) to predict Secchi depth from chlorophyll concentration and assuming that irradiance at Secchi depth was 15% of surface irradiance. In the channel, where suspended sediments dominated turbidity, we instead used the average attenuation coefficient of 1.5 observed on sampling dates 2 weeks prior to and after this study.  $I_0$  was estimated by interpolating irradiance estimates from hourly measurements from the California Irrigation Management Information System station at Twitchell Island, California (140) available at <http://www.cimis.water.ca.gov/> using a sine curve ( $r^2$  of predicted vs. observed >0.99). We used a conversion ratio of 2.07 to convert these data on full solar irradiance in units of  $\text{Watts m}^{-2}$  to PAR in  $\mu\text{mol quanta m}^{-2} \text{ s}^{-1}$  (Ting and Giacomelli 1987).  $U_{\max,t}^b$  and  $I_k$  for time points before the morning experiments and after the evening experiments were assumed to equal the values calculated from the corresponding experiments. We linearly interpolated between the morning and evening parameter values for the intervening time points. Integration over depth was accomplished numerically in Matlab (v. 5.3, MathSoft) using the quadrature method. Integration under the 24-h time series of depth-integrated uptake for each 0.1-h step was by the simple trapezoidal method. Shorter intervals between steps resulted in insignificant changes in integrated estimates.

We also made maximum and minimum estimates of daily areal phytoplankton and bacterial Se(IV) uptake. For the high-end estimate of phytoplankton Se(IV) uptake we subtracted the fraction of dark Se(IV) accounted for by particles <1.0  $\mu\text{m}$  from the dark Se(IV) uptake,  $y$ , before integrating

Eq. 1. This estimate assumes that all uptake >1.0 m was due to phytoplankton and that bacterial uptake was not related to light. The low end phytoplankton estimate was determined by setting  $y = 0$  in Eq. 1. This estimate assumes that all dark uptake is due to bacteria. Maximum and minimum estimates of bacterial Se(IV) uptake were determined by subtracting, respectively, the minimum and maximum phytoplankton Se(IV) uptake from total Se(IV) uptake.

To determine the uncertainty around our model estimates, 1000 sets of  $y$ ,  $U_{\max,t}^b$ , and  $I_k$  for Se(IV) and C uptake were produced by randomly sampling from normal distributions with means and standard deviations determined from the regressions of uptake on light. We then calculated the integrated primary production using each of these data sets and used the resulting distribution to estimate 5th and 95th percentiles for the estimates of daily areal production.

## Results

*Phytoplankton biomass and community composition*—The composition of the phytoplankton community differed between the Channel and Chl max sites, and over the course of the day at the Chl max site (Table 2). In the channel the biomass was dominated (>85%) by a small centric diatom, *Cyclotella atomus*, with smaller contributions by cryptophytes and cyanobacteria. At the Chl max site within Mildred Island, the cryptophytes were more important than in the channel, with the two genera *Plagioselmis* and *Teleaulax* comprising from 12% to 32% of the standing biovolume depending on the time of day. The cyanobacterium, *Cyanobium* sp. (1–2  $\mu\text{m} \times 4 \mu\text{m}$ ; Komárek 2003) also was more important at the Chl max site, comprising between 7% and 23% of the algal biovolume over 24 h. While the phytoplankton community composition varied significantly over the diel cycle, the composition between the two sampling times differed only modestly (Table 2).

*Se(IV) uptake*—Uptake of Se(IV) was approximately linear over the course of the incubations for all size fractions (Fig. 2). Because of this linearity we could calculate uptake rates simply based on  $^{75}\text{Se}$  in the particles at the end of the incubation. For the samples from the channel, less than 4% of the radiolabel was removed from solution over the entire course of the experiments and less than 12% was removed in the experiments using water from the Chl max site. The uptake rates of Se(IV) in the >0.2- $\mu\text{m}$  fractions were significantly related to light (Fig. 3, Table 3). The hyperbolic tangent model provided an excellent fit to the data from the

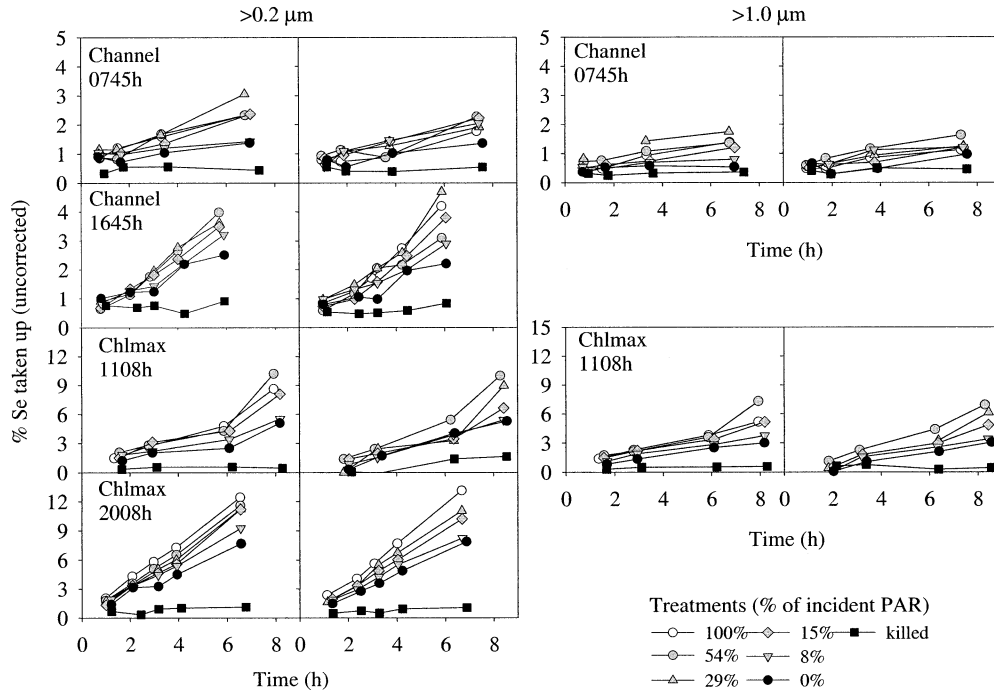


Fig. 2. Time series of <sup>75</sup>Se(IV) uptake for all experiments. Percentages given in legend are with reference to the irradiance in the chamber with the highest value. Side by side panels for each combination of time, site, and size fraction represent results for each replicate.

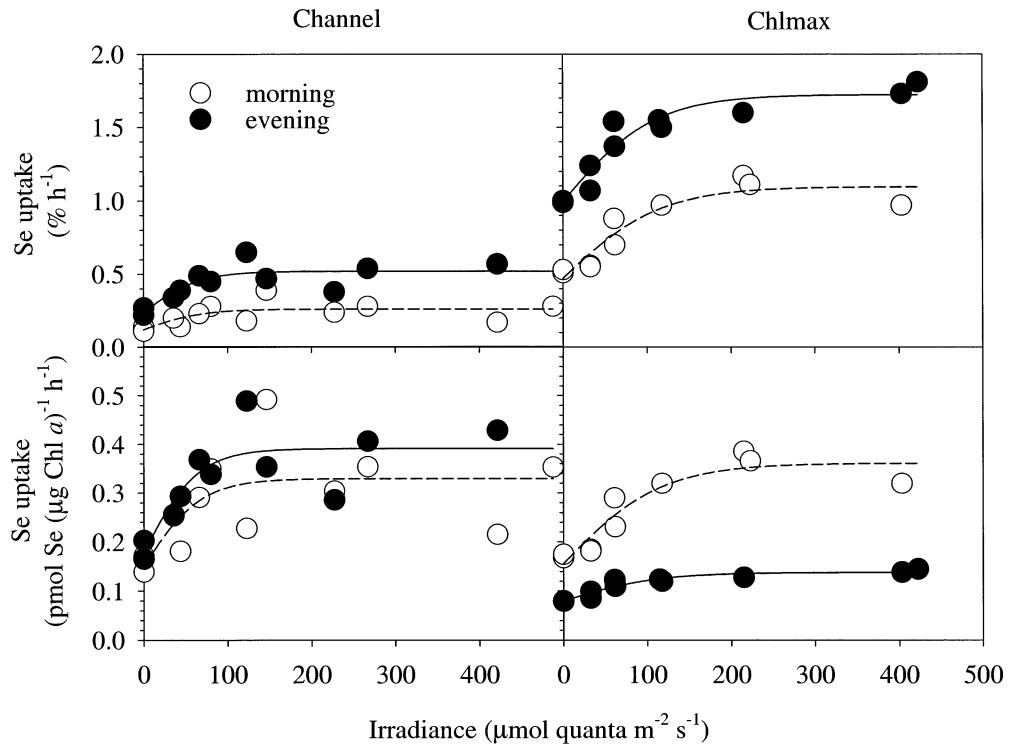


Fig. 3. Se(IV) uptake versus irradiance for the  $>0.2\text{-}\mu\text{m}$  fraction. Lines represent regression predictions based on hyperbolic tangent model. Broken lines are predictions for morning data, and solid lines for evening data. See Table 3 for parameter estimates and statistics.

Table 3. Parameters for regressions predicting Se(IV) uptake from irradiance for raw and chlorophyll normalized data.  $y_0$  is the intercept of the nonlinear regression and represents the regression estimate of dark Se(IV) uptake.  $uSe_{\max}$  represents the estimate of maximum Se(IV) uptake minus the Se(IV) uptake in the dark, and  $I_k$  is the irradiance at which uptake is 76% of the maximum.  $uSe_{\max}^b$  is  $uSe_{\max}$  normalized to chlorophyll concentration. Values for  $I_k$ ,  $r^2$ , and  $p$  are the same for raw and chlorophyll normalized data. Values in parentheses are standard errors. Asterisks denote  $p$  values: \*  $0.1 > p > 0.01$ ; \*\*  $0.01 > p > 0.001$ ; \*\*\*  $p < 0.001$ .

Site	Time	Size fraction	$I_k$	% Se(IV) $h^{-1}$		pmol Se(IV) $\mu g$ (Chl $a$ ) $^{-1} h^{-1}$		Adj $r^2$	$p$	
				$y_0$	$uSe_{\max}$	$y_0$	$uSe_{\max}^b$			
Channel	Morning	Total	68 (49)	0.12* (0.05)	0.14* (0.05)	0.15* (0.06)	0.18* (0.07)	0.34	0.06	
		>1.0	129* (46)	0.05** (0.01)	0.10*** (0.02)	0.06** (0.02)	0.13*** (0.02)	0.80	0.0015	
		0.2–1.0	43 (71)	0.7* (0.02)	0.04 (0.03)	0.09* (0.03)	0.05 (0.04)	0.00	0.44	
	Evening	Total	65* (30)	0.24** (0.05)	0.28** (0.06)	0.18** (0.04)	0.21** (0.05)	0.63	0.008	
		Morning	Total	116* (36)	0.47*** (0.06)	0.62*** (0.09)	0.16*** (0.014)	0.21** (0.03)	0.85	0.0005
			>1.0	101* (35)	0.28*** (0.06)	0.47*** (0.07)	0.09** (0.02)	0.15*** (0.02)	0.81	0.0013
Chlorophyll maximum	Morning	0.2–1.0	277 (226)	0.20*** (0.02)	0.20* (0.09)	0.07*** (0.01)	0.07 (0.03)	0.64	0.012	
		Evening	Total	109*** (25)	0.99*** (0.06)	0.73*** (0.08)	0.08*** (0.005)	0.07*** (0.007)	0.89	<0.0001

Chl max site ( $p < 0.01$ , Table 3). Data from the channel site did not fit the data as well, in large part because the relatively low counts in these samples increased our analytical error significantly. The analytical coefficient of variation (CV) after subtraction of the killed dark controls ranged for the channel samples from 5.4% to 16.5%, whereas the CVs for counts from the Chl max site were always <5%.

The spatial and temporal patterns of Se(IV) uptake were complex. Relative Se(IV) uptake rates (%  $h^{-1}$ ) were 3.3- to 3.9-fold higher at the Chl max site than in the channel (Fig. 3). The relative uptake rates were also about twofold higher on average in the evening than in the morning at both sites. However, when absolute Se(IV) uptake rates calculated based on ambient Se(IV) concentrations were normalized to chlorophyll  $a$ , they varied much less. The chlorophyll-specific Se(IV) uptake (pmol Se(IV) ( $\mu g$  Chl  $a$ ) $^{-1} h^{-1}$ ) was the same for both channel samples and the morning sample from the Chl max site, but threefold lower than the other samples in the evening sample from the Chl max site (Fig. 3).

For both sites and times a significant amount of the Se(IV) uptake occurred in the absence of light. Dark uptake represented from 42% to 56% of the maximal Se(IV) uptake, with the highest fraction being at the Chl max site during the evening (Table 3, Fig. 3). Dark relative Se(IV) uptake rates (%  $h^{-1}$ ) were approximately 4 times higher at the Chl max site than in the channel. At both sites, dark relative uptake rate approximately doubled between morning and evening, although this difference was only significant for the Chl max site ( $p < 0.001$ , two-tailed  $t$ -test). This increase mirrored the increase in chlorophyll from morning to evening at both sites (Table 1). Consequently, chlorophyll-normalized dark uptake was relatively uniform among sites and times (Table 3). Once again, only the evening sample from the Chl max site

exhibited a significant (twofold) difference from the other samples.

Much of the Se(IV) uptake occurred into the bacterial fraction (Fig. 4, Table 3). When averaged over all light levels, the bacterial size fraction accounted for  $49 \pm 11\%$  and  $34 \pm 6\%$  of the Se(IV) uptake in the channel and Chl max sites, respectively. Of the dark uptake, the bacterial size fraction accounted for 67% and 42%, respectively, at the two sites. Uptake into this size fraction was at best weakly related to light; no discernible relationship could be found at the channel site, whereas a slight but significant positive relationship was noted at the Chl max site. The large fraction of Se(IV) taken up into the bacterial size fraction probably contributed to the relatively weak relationships between light and total Se(IV) uptake in the channel. When bacterial uptake was removed and only the >1- $\mu m$  fraction considered, the dependence of Se(IV) uptake on light was much stronger than for Se(IV) uptake into all particles >0.2  $\mu m$  (Fig. 4).

The median daily areal Se(IV) uptake rates (5th–95th percentile) in the channel and the Chl max sites were 5.8 (4.1–7.4)  $\mu g m^{-2} d^{-1}$  and 26.0 (22.0–29.7)  $\mu g m^{-2} d^{-1}$ , respectively. Half or more of this uptake was associated with dark uptake or uptake into the bacterial size fraction. The same values for the >1.0- $\mu m$  size class were 2.8 (1.9–3.5)  $\mu g m^{-2} d^{-1}$  and 13.7 (11.8–15.8)  $\mu g m^{-2} d^{-1}$ , or 45% and 53% of the total uptake. When all dark Se(IV) uptake was subtracted from total uptake, the daily integrated rates were 1.3 (0.7–1.9) and 2.4 (1.7–3.2) in the channel and the Chl max sites, or only 22% and 18% of total Se(IV) uptake.

*Carbon fixation*—The fixation of C into the >0.2- $\mu m$  fraction exhibited the typical relationship to light (Fig. 5, Table 4). Except for the evening experiment in the channel,

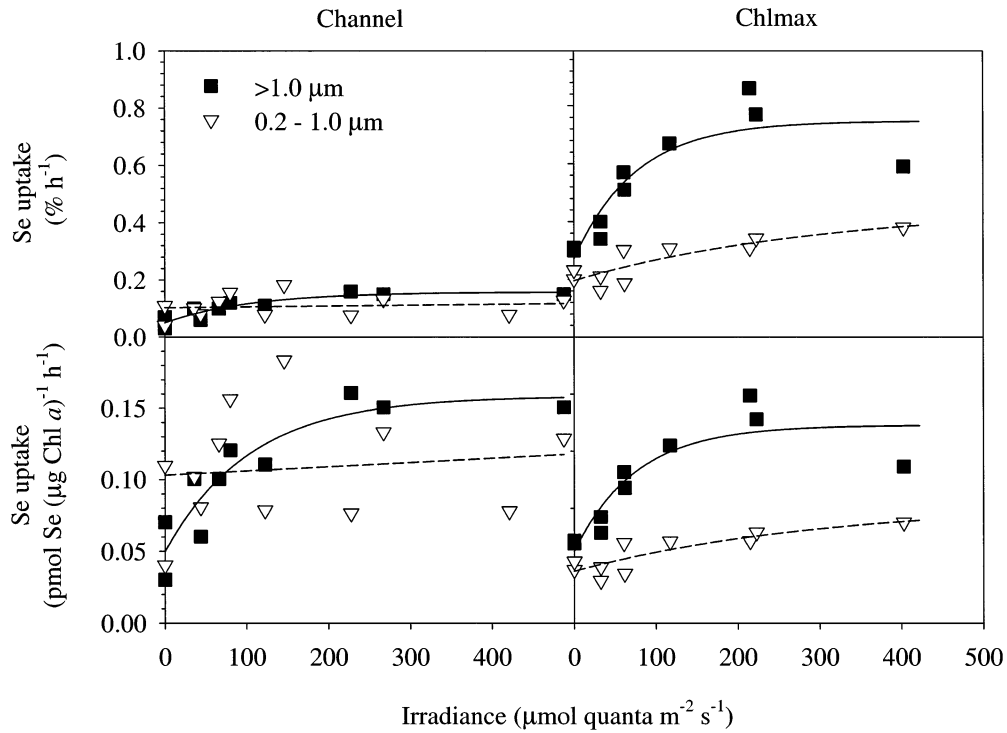


Fig. 4. Se(IV) uptake versus irradiance for the 0.2–1.0- $\mu\text{m}$  and  $>1.0\text{-}\mu\text{m}$  size fractions. Lines represent regression predictions. Solid lines are predictions for the  $>1.0\text{-}\mu\text{m}$  fraction and broken lines are predictions for the bacterial size fraction. Fitted parameters, standard deviations, and regression statistics are presented in Table 3.

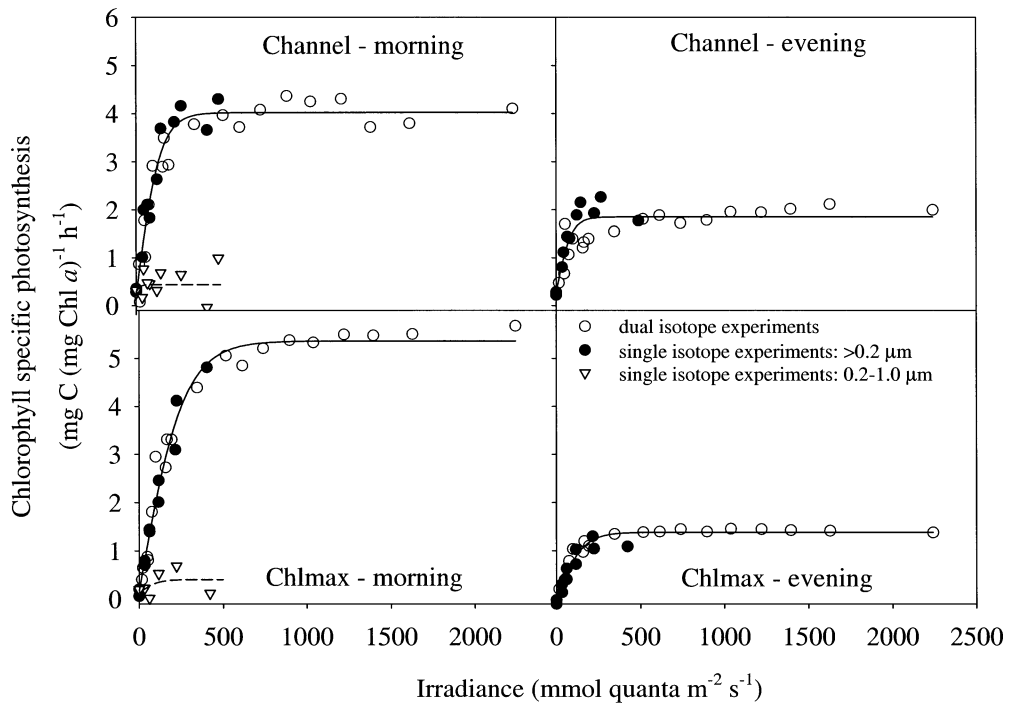


Fig. 5. Photosynthesis irradiance curves. Solid lines are the predictions of the hyperbolic tangent model fit to the data for particles  $>0.2\text{ }\mu\text{m}$  in size, and broken lines are the predictions for the 0.2–1.0- $\mu\text{m}$  fraction. Fitted parameters, standard deviations, and regression statistics are presented in Table 4.

Table 4. Parameters for models predicting chlorophyll-specific primary production from irradiance. Parameters are as described in Table 3 except that  $P_{\max}^b$  is the chlorophyll-specific maximum production minus dark production. Values in parentheses are standard errors. Asterisks denote parameters with  $p$  values  $<0.001$ ;  $p$  values for all other parameter estimates are  $>0.1$ .

Site	Time	Fraction ( $\mu\text{m}$ )	$n$	$y_0$	$P_{\max}^b$	$I_{95}$	Adj $r^2$	$p$
Channel	Morning	Total	31	0.23 (0.18)	3.79*** (0.19)	259*** (27)	0.93	$<0.0001$
		0.2–1.0	12	0.29 (0.27)	0.15 (0.03)	26 (324)	0.00	0.88
Channel	Evening	Total	29	0.27 (0.14)	1.59*** (0.18)	165*** (33)	0.76	$<0.0001$
		0.2–1.0	6	0.13 (0.28)	0.28 (0.33)	270 (487)	0.00	0.73
Chlorophyll maximum	Morning	Total	30	0.17 (0.12)	5.19*** (0.14)	488*** (31)	0.98	$<0.0001$
		0.2–1.0	6	0.13 (0.28)	0.28 (0.33)	270 (487)	0.00	0.73
Chlorophyll maximum	Evening	Total	30	0.0 (0.08)	1.38*** (0.09)	263*** (31)	0.91	$<0.0001$

the data from the dual isotope and the single isotope experiments agreed well. As expected based on the 5.4- to 9.7-fold difference in chlorophyll concentrations between the sites, maximum C fixation rates were 7.3- to 8.4-fold higher at the Chl max site than in the channel. However, C fixation at saturating light intensity in the evening at both sites was 56–64% of that in the morning, even though chlorophyll concentrations were higher in the evening. Consequently, the maximum chlorophyll-specific primary production ( $P_{\max}^b$ ) declined from morning to evening by 2.4-fold in the channel

and over 3.8-fold at the Chl max site (Fig. 5;  $p < 0.0001$  for both comparisons; two-tailed  $t$ -test).

The median (5th–95th percentiles) daily areal primary production was 1.25 (0.89–1.62)  $\text{g C m}^{-2} \text{d}^{-1}$  at the Chl max site and 0.26 (0.19–0.33)  $\text{g C m}^{-2} \text{d}^{-1}$  in the channel. C fixation into the 0.2–1.0- $\mu\text{m}$  fraction did not vary significantly with light (Table 4, Fig. 5). Chlorophyll-specific primary production in this fraction in the channel averaged 0.48  $\mu\text{g C } (\mu\text{g Chl } a)^{-1} \text{h}^{-1}$  (standard error [SE] = 0.11,  $n = 12$ ), or 13% of  $P_{\max}^b$ ; the same parameter for the Chl max site was 0.33  $\mu\text{g C } (\mu\text{g Chl } a)^{-1} \text{h}^{-1}$  (SE = 0.10,  $n = 6$ ), or 6% of  $P_{\max}^b$ .

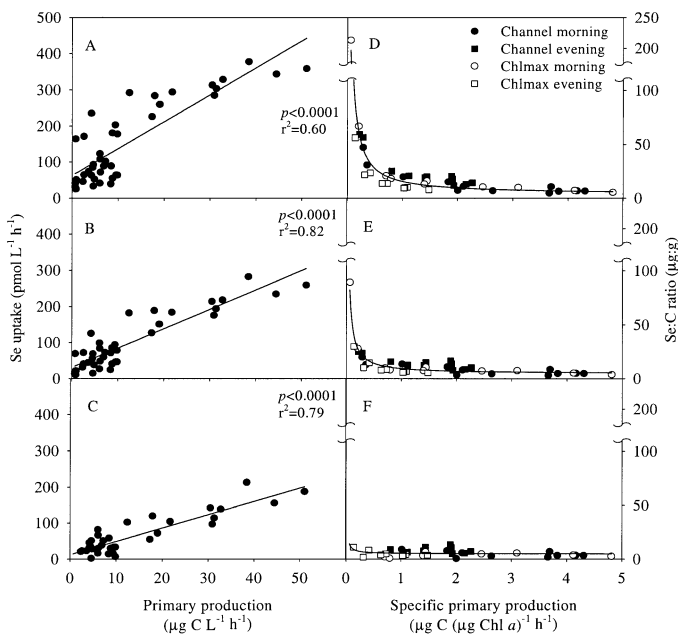


Fig. 6. Dependence of Se(IV):C uptake ratios on C uptake based on the dual isotope experiments. Panels A–C depict the relationship between Se(IV) uptake and primary production, and panels D–F show the relationship between the Se(IV):C uptake ratio and chlorophyll-specific primary productivity. Panels A and D relate to total Se(IV) uptake, panels B and E to the Se(IV) uptake exclusive of uptake into the 0.2–1.0- $\mu\text{m}$  fraction, and panels C and F to Se(IV) uptake exclusive of dark uptake.

*Relationships between C and Se(IV) uptake*—Se(IV) uptake is more tightly coupled with C uptake than with irradiance when all the data are pooled. While Se(IV) and inorganic C uptake displayed similar relationships to irradiance within a sample, the slopes and intercepts of the nonlinear relations between Se(IV) and C uptake and irradiance vary significantly among sites and sampling times. Consequently, when all data are pooled, the relation between Se(IV) uptake and irradiance is insignificant ( $r^2 = 0.02$ ,  $p = 0.31$ ,  $n = 55$ ), whereas Se(IV) uptake is significantly related to C fixation (Fig. 6A;  $r^2 = 0.61$ ,  $p < 0.0001$ ,  $n = 55$ ). The fit of the linear relationship between C uptake and Se(IV) uptake improved when Se(IV) uptake into the 0.2–1.0- $\mu\text{m}$  fraction (Fig. 6B;  $r^2 = 0.82$ ) or dark uptake (Fig. 6C;  $r^2 = 0.79$ ) was subtracted from total Se(IV) uptake. The same corrections improve the  $r^2$  of the relationship between irradiance and Se(IV) uptake to only 0.07 and 0.10, respectively.

Bacterial and dark uptake account for nearly all of the spatial and temporal variability in the Se(IV):C uptake ratio. Analysis of covariance (ANCOVA) indicates significant differences in Se(IV) uptake between the sites and sampling times that are not accounted for by the regression of total Se(IV) uptake on C uptake (Table 5). However, if uptake of Se(IV) into the bacterial fraction is subtracted from total Se(IV) uptake, these differences are reduced. When dark Se(IV) uptake is subtracted from total Se(IV) uptake, all dif-

Table 5. Results of the analysis of covariance that characterizes the regression of Se(IV) uptake on primary production and estimates the fixed residual differences in Se(IV) uptake between sites and sampling times.  $A$  and  $y_0$  are the slope and intercept, respectively, of the linear regression. The class terms site and time are the mean residual differences between the sites (Channel – Chl max) and sampling times (evening – morning). Interaction effects were never significant. RMSE = root mean square error of the ANCOVA. The results under Seston are based on Se(IV) uptake for all particles  $>0.2 \mu\text{m}$ . The results for the Phytoplankton are based either on Se(IV) uptake into the  $>1.0 \mu\text{m}$  fraction, or Se(IV) uptake into the  $>0.2 \mu\text{m}$  fraction corrected for dark uptake.

	Seston (al Se(IV) uptake)			Phytoplankton					
				$>1.0 \mu\text{m}$ Se(IV) uptake			No dark Se(IV) uptake		
	Estimate	SE	$p$	Estimate	SE	$p$	Estimate	SE	$p$
$y_0$	113	6.0	$<0.0001$	62.7	6.02	$<0.0001$	10.4	7.9	0.20
$A$	4.07	0.37	$<0.0001$	4.07	0.37	$<0.0001$	4.6	0.31	$<0.0001$
Site	-67	4.7	$<0.0001$	-42	4.7	0.02	2.1	5.8	0.27
Time	14	3.6	0.0004	8.8	3.6	0.33	1.5	4.2	0.72
$n$	41			41			35		
Adj $r^2$	0.96			0.93			0.79		
RMSE	22.7			1.71			24.4		
Model $p$	$<0.0001$			$<0.0001$			$<0.0001$		

ferences between sites and times become insignificant ( $p > 0.2$ ). Moreover, the intercept of the regression becomes indistinguishable from 0, which indicates (based on the regression slope) a proportional uptake of Se(IV) and C of  $4.6 \pm 0.31 \mu\text{g Se g C}^{-1}$  that is consistent between sites and times. This is made clearer by inspecting the relationship between the Se(IV):C uptake ratio and primary production. Because some Se(IV) uptake occurs in the dark when C uptake is negligible, the relationship between C fixation and the Se(IV):C uptake ratio is negative and nonlinear (Fig. 6D). The nonlinear relationship between the Se(IV):C uptake ratio and C fixation is much reduced when Se(IV) uptake into the 0.1–1.0- $\mu\text{m}$  fraction is subtracted from total Se(IV) uptake (Fig. 6E). The nonlinearity is eliminated entirely by subtracting dark Se(IV) uptake from total Se(IV) uptake, indicating that the nonlinearity is entirely due to dark uptake (Fig. 6F).

## Discussion

*Coupling of C and Se(IV) uptake*—The correlations between C and Se(IV) uptake suggest that Se accumulation by algae is closely tied to the fixation of organic matter and cell growth. Similar observations have been made for cultured algae where uptake of Se(IV) and cell growth is also correlated as long as Se(IV) is not depleted (Baines and Fisher 2001). Regulation of Se(IV) uptake is also clearly indicated by measurements of Se:C in the seston during our experiments (M. Doblin pers comm.). Since selenium within the cell is primarily covalently bound in proteins and amino acids (Wrench 1978; Bottino et al. 1984; Vandermeulen and Foda 1988; Fisher and Reinfelder 1991), and these molecules are fundamental to cell function, it is likely that their synthesis is regulated, resulting in the strong relationship between Se(IV) and C.

While the overall correlation between Se(IV) and C uptake suggests a strong linkage between the two processes, the existence of significant Se(IV) uptake in the dark partially decouples the two processes in time and space, thereby adding noise to the correlation between Se(IV) and C uptake.

In fact, 75–85% of the daily areal Se(IV) uptake is not related to light, since the dark uptake occurs throughout the day and throughout the water column, whereas the light-associated uptake occurs mostly near the surface and only during the day. If Se(IV) uptake and Se(IV):C uptake ratios are to be modeled properly, this dark Se(IV) uptake must be accounted for. Dark Se(IV) uptake could result from either phytoplankton or bacterial activity. Temporal uncoupling of protein synthesis and sulfur uptake from photosynthesis has been previously observed in situ (Cuhel et al. 1982). Thus, algal cells may be producing Se-containing proteins in the dark using energy and C fixed into carbohydrates in the light. However, heterotrophic bacteria may also contribute significantly to in situ dark Se(IV) uptake (Foda et al. 1983; Riedel et al. 1996). (Note that the dominant cyanobacterium, *Cyanobium* sp., is 1–2  $\times$  4  $\mu\text{m}$  and, thus, likely captured in the  $>1\text{-}\mu\text{m}$  algal fraction.) We have direct support for this hypothesis, since about half of the dark Se(IV) uptake in the morning experiments occurred in the 0.2–1.0- $\mu\text{m}$  size fraction (Fig. 4). Moreover, up to half of the heterotrophic bacterial activity in eutrophic freshwater ecosystems can be found in the  $>1\text{-}\mu\text{m}$  fraction (Riemann et al. 1982), so a great deal more dark Se(IV) uptake by heterotrophic bacteria may have occurred in larger size classes. Thus, while a fraction of the Se(IV) uptake may reflect dark uptake by phytoplankton, most of the dark Se(IV) uptake may be attributable to bacteria.

The two to fourfold decline in photosynthetic efficiency from morning to evening caused Se(IV):C uptake ratios to increase over the course of the day (see Time effect in Table 5). It is very unlikely that the modest changes in algal species composition between sampling times could cause such a large change in themselves (Table 2). Moreover, the onset of P or N limitation is unlikely because ambient levels of these nutrients were never low enough to be limiting ( $[\text{NO}_3^-] = 20\text{--}22 \mu\text{mol L}^{-1}$ ;  $[\text{PO}_4^{3-}] = 1.7\text{--}2.1 \mu\text{mol L}^{-1}$ ;  $[\text{SiO}_4^-] = 240\text{--}260 \mu\text{mol L}^{-1}$ ). Instead, the decrease in photosynthetic efficiency may have resulted from temporary C limitation. The strong C demand by algae is indicated by the DIC decline from 1  $\text{mmol L}^{-1}$  to 0.6  $\text{mmol L}^{-1}$  over the

course of the day (Table 1). In similarly productive freshwater environments, high rates of C fixation can temporarily deplete the aqueous  $\text{CO}_2$  and outstrip the rate of dissociation of  $\text{CO}_2$  from  $\text{HCO}_3^-$  and influx from the atmosphere with the result being reduced photosynthesis (Hein 1997; Ibelings and Maberly 1998). In any case, the effect of lower evening photosynthetic efficiency on  $\text{Se(IV)}:\text{C}$  uptake ratios at our sites is modest and is not evident at all after  $\text{Se(IV)}$  uptake is corrected for bacterial and dark uptake.

**Comparisons to particulate  $\text{Se}:\text{C}$** —A direct comparison of the  $\text{Se(IV)}:\text{C}$  uptake ratios with the  $\text{Se}:\text{C}$  ratio in suspended particles at the Chl max site, where algal biomass dominated the seston, would indicate to what degree our  $\text{Se(IV)}$ -based radiotracer method quantified the major pathways of Se uptake. The residence time at the Chl max site is very long compared to most other sites in the delta, allowing phytoplankton biomass to accumulate (Lucas et al. 2002). Also in contrast to other sites in the delta, there is little evidence of sediment resuspension in this part of Mildred Island (G. Cutter and L. Cutter pers. comm.). Based on our measurements of particulate organic carbon (POC) and chlorophyll *a* concentrations and assuming a  $\text{C}:\text{Chl}$  value of 27.8 (Cloern et al. 1995), we estimate that algal biomass amounted to 53% ( $\pm 11\%$ ) of the total POC. At the channel site the same value was 21% ( $\pm 5\%$ ). Assuming that bacterial biomass is approximately 32.5% of algal biomass in delta shallow water habitats (Sobczak et al. 2002),  $\sim 70\%$  the POC at the Chl max was comprised of living bacterial and algal cells.

To make an appropriate comparison between the  $\text{Se}:\text{C}$  ratios measured using chemical and radiotracer methods, we must first account for the contribution of bacteria to particulate organic carbon production. Past work has shown that bacterial production in Mildred Island and another flooded island, Frank's Tract, averaged 29.3%  $\pm 5.7\%$  of primary production ( $n = 18$ ; Sobczak et al. 2002). Two independent lines of reasoning suggest that this value is reasonable. First, it is very similar to the median percentage of primary production represented by bacterial production of 26.5% observed by Cole et al. (1988) when comparing a wide range of aquatic ecosystems. Second, it conforms to energetic constraints. If one assumes a bacterial growth efficiency of 50% in this system, this estimate of bacterial production implies a bacterial carbon requirement equivalent to  $\sim 60\%$  of primary production. Since a bacterial growth efficiency of 50% is at the high end of the observed range (del Giorgio and Cole 1998), the real bacterial carbon requirement may be an even greater proportion of primary production, leaving less than 40% of the primary production for grazing, sinking, and advective losses. Consequently, at least for the Chl max site where local biological production easily outpaces advective loss, higher bacterial production would cause the C budget to be unbalanced.

After accounting for bacterial uptake, the total plankton  $\text{Se(IV)}:\text{C}$  average uptake ratio for the Chl max site was 15.9  $\mu\text{g Se g C}^{-1}$ , which is about 30% higher than the average  $\text{Se}:\text{C}$  ratio of 12.05  $\mu\text{g Se g C}^{-1}$  measured in particulate matter  $>0.45 \mu\text{m}$  (Fig. 7). However, the uptake ratio falls within the range of measured particulate  $\text{Se}:\text{C}$  and the av-

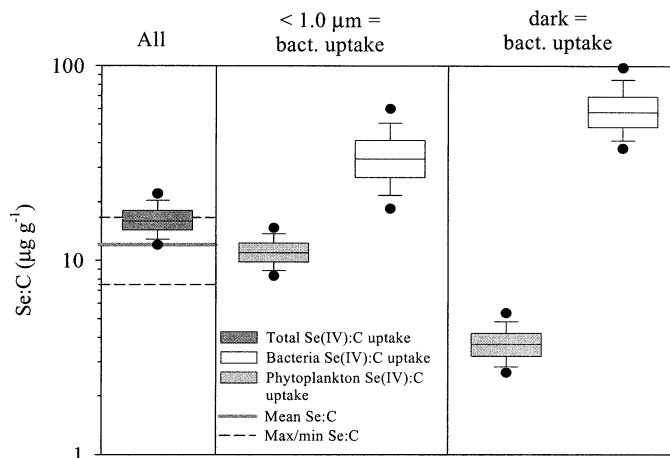


Fig. 7. Box plots of  $\text{Se(IV)}:\text{C}$  uptake ratios for all seston, phytoplankton, and bacteria at the Chl max site. The lines represent the median value. The boxes span the 25th and 75th percentiles, the whiskers the 10th and 90th percentiles, and the round symbols the 5th and 95th percentiles. The thick gray line is the mean of  $\text{Se}:\text{C}$  estimates for the  $>0.45\text{-}\mu\text{m}$  seston at the Chl max site, and the broken lines are the maximum and minimum for the diel series.

erage  $\text{Se}:\text{C}$  ratio is between the 5th and the 95th percentiles of the uptake ratio estimates. The relatively close agreement between the measurements of  $\text{Se(IV)}:\text{C}$  uptake ratios and measured  $\text{Se}:\text{C}$  is intriguing given that significant uptake of dissolved organic  $\text{Se(-II)}$  by phytoplankton and bacteria in this system is suggested both by direct uptake of dissolved  $\text{Se(-II)}$  in cultured algae (Baines et al. 2001) and by strong diel fluctuations in dissolved and particulate Se pools at the Chl max site (M. Doblin pers. comm.). The agreement between the  $\text{Se(IV)}:\text{C}$  uptake ratios estimated from our radioisotope experiments and suspended measurements of particulate  $\text{Se}:\text{C}$  may be explained if exchanging extracellular and intracellular Se pools were turned over quickly relative to the 6–8-h experimental period. Such turnover would allow the intracellular and extracellular  $\text{Se(-II)}$  pools to reach isotopic equilibration with the dissolved  $\text{Se(IV)}$  pool. As a consequence, the radioisotope experiments would measure net uptake of both dissolved  $\text{Se(IV)}$  and  $\text{Se(-II)}$  rather than the net uptake of  $\text{Se(IV)}$  alone. This issue is dealt with more completely in a separate paper (M. Doblin pers. comm.).

Our results suggest that a simpler method for measuring  $\text{Se(IV)}$  uptake using radiotracers may be possible. Separately modeling the response of  $\text{Se(IV)}$  uptake to light is a difficult process because of the number of points required to adequately fit a nonlinear equation and because the low radioactivity in these experiments (necessitated by the need to add label at tracer levels) results in larger volumes of sample to filter, longer incubation periods, and longer analysis times. The process may be simplified by recognizing that  $\text{Se(IV)}$  uptake at a particular site consists of two basic components, one that is related to light and characterized by a relatively fixed ratio to primary production and another that occurs in the dark and is therefore independent of primary production. To derive the relationship between  $\text{Se(IV)}$  uptake and irradiance, we need only estimate the dark  $\text{Se(IV)}$  uptake at a site, the dark corrected  $\text{Se(IV)}:\text{C}$  uptake ratio at a saturating

irradiance value (to maximize the signal) and the photosynthesis:irradiance curve. The product of the latter two elements yields the light-dependent portion of the Se(IV) to irradiance curve, while the dark uptake provides the y-intercept of that relationship. This equation can then be integrated over time and depth. By focusing effort on only two points in the Se(IV) uptake:irradiance curve, it should be possible to more efficiently determine the Se(IV):C uptake ratio. The contribution of bacteria to C fixation can be assessed by measuring bacterial production directly.

*Se:C in phytoplankton and bacteria*—Given that bacterial production at the Chl max site is likely to amount to only a fraction of primary production, the observed predominance of Se(IV) uptake into small particles and in the dark suggests that bacteria may have a higher Se(IV):C uptake ratio than do phytoplankton. By assuming (1) that Se(IV) uptake into particles  $<1.0 \mu\text{m}$  is a minimum estimate of bacterial Se(IV) uptake, (2) that dark Se(IV) uptake is a maximum estimate of bacterial Se(IV) uptake, and (3) that daily areal bacterial production is  $29.3\% \pm 5.7\%$  of primary production, we can bracket the range of possible bacterial Se(IV):C uptake ratios (Sobczak et al. 2002). These estimates can then be compared to maximum and minimum phytoplankton Se(IV):C uptake ratios based on the same assumptions.

In all cases and for all scenarios, the bacterial Se(IV):C uptake ratios were significantly larger than those for phytoplankton (Fig. 7). Under the assumption that only uptake  $<1.0 \mu\text{m}$  was due to bacteria, the bacterial Se(IV):C uptake ratio was 2.4-fold larger than the phytoplankton Se(IV):C estimate. Only 32 of the 1000 random sets of parameters produced the bacterial Se(IV):C ratios that were larger than the phytoplankton Se(IV):C ratio. If we assume that all dark Se(IV) uptake is due to bacteria, the Se(IV):C uptake ratio for bacteria becomes more than an order of magnitude larger than the phytoplankton value. Bacteria do not typically constitute a large proportion of the POC in the water column of this ecosystem, and they are even less important as a source of energy to higher trophic levels (Sobczak et al. 2002). However, by virtue of their high Se(IV):C uptake ratios, bacteria may contribute significantly to Se trophic transfer to consumers. Consumers that directly or indirectly depend more upon bacteria for carbon and energy may thus be exposed to more Se through their diet. Moreover, spatial or temporal variability in the relative importance of bacteria and phytoplankton as carbon sources could generate corresponding patterns in consumer Se tissue concentrations.

Dual radiotracer uptake experiments can provide valuable information that, in combination with direct measurements of dissolved and particulate Se and C, allows us to elucidate mechanisms and rates of Se transformation in natural ecosystems. We used such experiments to study coupled Se and C dynamics in a riverine channel environment and a site with a longer hydraulic residence time. We showed that Se(IV) and C uptake into suspended particles exhibits very similar relationships to light, although a significant amount of Se(IV) uptake occurred in the dark. Moreover, bacteria are responsible for much of the Se(IV) uptake into particles in this system. Measurements of Se:C ratios in newly produced organic material that were based on the Se(IV) and C uptake

experiments agreed well with direct observations of Se:C at a site where the suspended organic matter was dominated by phytoplankton biomass. These measurements also indicated that bacteria appear to possess much higher Se:C ratios than do phytoplankton in this ecosystem. Consequently, the diet of consumers and local or temporal variations in the relative contribution of algae and bacteria to seston may have a large impact on Se concentrations in consumers.

## References

- ARAR, E. J., AND G. B. COLLINS. 1997. Method 445.0: *In vitro* determination of chlorophyll *a* and pheophytin *a* in marine and freshwater algae by fluorescence. National Exposure Research Laboratory, Office of Research and Development, U.S. Environmental Protection Agency.
- BAINES, S. B., AND N. S. FISHER. 2001. Interspecific differences in the bioconcentration of selenite by phytoplankton and their ecological implications. *Mar. Ecol. Prog. Ser.* **213**: 1–12.
- , ———, M. A. DOBLIN, AND G. A. CUTTER. 2001. Uptake of dissolved organic selenides by marine phytoplankton. *Limnol. Oceanogr.* **46**: 1936–1944.
- , ———, AND R. STEWART. 2002. Assimilation and retention of selenium and other trace elements from crustacean food by juvenile striped bass (*Morone saxatilis*). *Limnol. Oceanogr.* **47**: 646–655.
- BOTTINO, N. R., C. H. BANKS, K. J. IRGOLIC, P. MICKS, A. E. WHEELER, AND R. A. ZINGARO. 1984. Selenium containing amino-acids and proteins in marine-algae. *Phytochemistry* **23**: 2445–2452.
- BOWIE, G. L., AND OTHERS. 1996. Assessing selenium cycling and accumulation in aquatic ecosystems. *Water Air Soil Poll.* **90**: 93–104.
- BROWN, T. A., AND A. SHRIFT. 1982. Selenium—toxicity and tolerance in higher plants. *Biol. Rev. Cambridge Philos. Soc.* **57**: 59–84.
- CARLSON, R. E. 1977. Trophic state index for lakes. *Limnol. Oceanogr.* **22**: 361–369.
- CLOERN, J. E., C. GRENZ, AND L. VIDERGARLUCAS. 1995. An empirical model of the phytoplankton chlorophyll:carbon ratio—The conversion factor between productivity and growth rate. *Limnol. Oceanogr.* **40**: 1313–1321.
- COLE, J. J., S. FINDLAY, AND M. L. PACE. 1988. Bacterial production in fresh and saltwater ecosystems—a cross-system overview. *Mar. Ecol. Prog. Ser.* **43**: 1–10.
- CUHEL, R. L., C. D. TAYLOR, AND H. W. JANNASCH. 1982. Assimilatory sulfur metabolism in marine microorganisms—considerations for the application of sulfate incorporation into protein as a measurement of natural-population protein-synthesis. *Appl. Environ. Microbiol.* **43**: 160–168.
- CUTTER, G. A. 1978. Species determination of selenium in natural waters. *Anal. Chim. Acta* **98**: 59–66.
- . 1982. Selenium in reducing waters. *Science* **217**: 829–831.
- . 1983. Elimination of nitrite interference in the determination of selenium by hydride generation. *Anal. Chim. Acta* **149**: 391–394.
- . 1985. Determination of selenium speciation in biogenic particulate material and sediments. *Anal. Chem.* **57**: 2951–2955.
- , AND L. S. CUTTER. 1998. Metalloids in the high latitude north Atlantic Ocean: Sources and internal cycling. *Mar. Chem.* **61**: 25–36.
- , AND J. RADFORD-KNOERY. 1991. Determination of carbon, nitrogen, sulfur, and inorganic sulfur species in marine particles, pp. 57–63. *In* D. Hurd and D. Spencer [eds.], *Marine*

- particles: Analysis and characterization. American Geophysical Union.
- DEL GIORGIO, P. A., AND J. J. COLE. 1998. Bacterial growth efficiency in natural aquatic systems. *Ann. Rev. Ecol. Syst.* **29**: 503–541.
- FALKOWSKI, P. G., AND J. A. RAVEN. 1997. Aquatic photosynthesis. Blackwell Science.
- FINDLAY, S., M. L. PACE, D. LINTS, J. J. COLE, N. F. CARACO, AND B. PEIERLS. 1991. Weak-coupling of bacterial and algal production in a heterotrophic ecosystem—the Hudson River Estuary. *Limnol. Oceanogr.* **36**: 268–278.
- FISHER, N. S., AND J. R. REINFELDER. 1991. Assimilation of selenium in the marine copepod *Acartia tonsa* studied with a radiotracer ratio method. *Mar. Ecol. Prog. Ser.* **70**: 157–164.
- , AND ———. 1995. The trophic transfer of metals in marine systems, pp. 363–406. *In* A. Tessier and D. R. Turner [eds.], Metal speciation and bioavailability in aquatic systems. Wiley and Sons.
- FODA, A., J. H. VANDERMEULEN, AND J. J. WRENCH. 1983. Uptake and conversion of selenium by a marine bacterium. *Can. J. Fish. Aquat. Sci.* **40**: 215–220.
- FURUTANI, A., J. W. M. RUDD, AND C. A. KELLY. 1984. A method for measuring the response of sediment microbial communities to environmental perturbations. *Can. J. Microbiol.* **30**: 1408–1414.
- HARRISON, P. J., P. W. YU, P. A. THOMPSON, N. M. PRICE, AND D. J. PHILLIPS. 1988. Survey of selenium requirements in marine-phytoplankton. *Mar. Ecol. Prog. Ser.* **47**: 89–96.
- HEIN, M. 1997. Inorganic carbon limitation of photosynthesis in lake phytoplankton. *Freshwat. Biol.* **37**: 545–552.
- HU, M. H., Y. P. YANG, J. M. MARTIN, K. YIN, AND P. J. HARRISON. 1997. Preferential uptake of Se(IV) over Se(VI) and the production of dissolved organic Se by marine phytoplankton. *Mar. Environ. Res.* **44**: 225–231.
- IBELINGS, B. W., AND S. C. MABERLY. 1998. Photoinhibition and the availability of inorganic carbon restrict photosynthesis by surface blooms of cyanobacteria. *Limnol. Oceanogr.* **43**: 408–419.
- JASSBY, A. D., AND T. PLATT. 1976. Mathematical formulation of the relationship between photosynthesis and light for the phytoplankton. *Limnol. Oceanogr.* **21**: 540–547.
- KELLER, M. D., W. K. BELLOWS, AND R. R. L. GUILLARD. 1988. Microwave treatment for sterilization of phytoplankton culture media. *J. Exp. Mar. Biol. Ecol.* **117**: 279–283.
- KOMÁREK, J. 2003. Coccoid and colonial cyanobacteria, p. 59–116. *In* J. Wehr and R. Sheath [eds.], *Freshwater Algae of North America: Ecology and Classification*. Academic Press.
- LAUHLI, A. 1993. Selenium in plants—uptake, functions, and environmental toxicity. *Bot. Acta* **106**: 455–468.
- LEWIS, M. R., AND J. C. SMITH. 1983. A small volume, short-incubation-time method for measurement of photosynthesis as a function of incident irradiance. *Mar. Ecol. Prog. Ser.* **13**: 99–102.
- LIU, D. L., Y. P. YANG, M. H. HU, P. J. HARRISON, AND N. M. PRICE. 1987. Selenium content of marine food-chain organisms from the coast of China. *Mar. Environ. Res.* **22**: 151–165.
- LUCAS, L. V., J. E. CLOERN, J. K. THOMPSON, AND N. E. MONSEN. 2002. Functional variability of habitats within the Sacramento–San Joaquin Delta: Restoration implications. *Ecol. Appl.* **12**: 1528–1547.
- LUOMA, S. N., C. JOHNS, N. S. FISHER, N. STEINBERG, R. OREMLAND, AND J. R. REINFELDER. 1992. Determination of selenium bioavailability to a benthic bivalve from particulate and solute pathways. *Environ. Sci. Technol.* **26**: 485–491.
- MONSEN, N. E., J. E. CLOERN, L. V. LUCAS, AND S. G. MONISMITH. 2002. A comment on the use of flushing time, residence time, and age as transport time scales. *Limnol. Oceanogr.* **47**: 1545–1553.
- PRESSER, T. S. 1994. The Kesterson effect. *Environ. Manag.* **18**: 437–454.
- , M. A. SYLVESTER, AND W. H. LOW. 1994. Bioaccumulation of selenium from natural geologic sources in western states and its potential consequences. *Environ. Manag.* **18**: 423–436.
- REINFELDER, J. R., AND N. S. FISHER. 1991. The assimilation of elements ingested by marine copepods. *Science* **251**: 794–796.
- , ———, S. N. LUOMA, J. W. NICHOLS, AND W. X. WANG. 1998. Trace element trophic transfer in aquatic organisms: A critique of the kinetic model approach. *Sci. Total Environ.* **219**: 117–135.
- RIEDEL, G., D. FERRIER, AND J. SANDERS. 1991. Uptake of selenium by fresh-water phytoplankton. *Water Air Soil Poll.* **57**: 23–30.
- , AND J. G. SANDERS. 1996. The influence of pH and media composition on the uptake of inorganic selenium by *Chlamydomonas reinhardtii*. *Environ. Toxicol. Chem.* **15**: 1577–1583.
- , ———, AND C. C. GILMOUR. 1996. Uptake, transformation, and impact of selenium in freshwater phytoplankton and bacterioplankton communities. *Aquat. Microb. Ecol.* **11**: 43–51.
- RIEMANN, B., AND OTHERS. 1982. Carbon metabolism during a spring diatom bloom in the eutrophic Lake Mossø. *Int. Rev. Gesamten Hydrobiol.* **67**: 145–185.
- SOBCZAK, W. V., J. E. CLOERN, A. D. JASSBY, AND A. B. MULLER-SOLGER. 2002. Bioavailability of organic matter in a highly disturbed estuary: The role of detrital and algal resources. *Proc. Natl. Acad. Sci. U.S.A.* **99**: 8101–8105.
- STERNER, R. W., AND J. J. ELSER. 2002. *Ecological stoichiometry*. Princeton Univ. Press.
- TING, K. C., AND G. A. GIACOMELLI. 1987. Availability of solar photosynthetically active radiation. *Trans. ASAE* **30**: 1453–1457.
- VANDERMEULEN, J., AND A. FODA. 1988. Cycling of selenite and selenate in marine phytoplankton. *Mar. Biol.* **98**: 115–123.
- WANG, W. X., N. S. FISHER, AND S. N. LUOMA. 1996. Kinetic determinations of trace element bioaccumulation in the mussel *Mytilus edulis*. *Mar. Ecol. Prog. Ser.* **140**: 91–113.
- WRENCH, J. J. 1978. Selenium metabolism in marine phytoplankters *Tetraselmis tetrathele* and *Dunaliella minuta*. *Mar. Biol.* **49**: 231–236.

Received: 2 June 2002

Accepted: 26 October 2003

Amended: 3 November 2003